September 16, 2007

Terahertz quantum-cascade lasers with resonant-phonon depopulation: high-temperature and low-frequency operation

Sushil Kumar, Benjamin S. Williams*, Qi Qin, Alan W. M. Lee and Qing Hu (MIT, USA)

John L. Reno (Sandia National Laboratories, USA)

Z. R. Wasilewski, and H. C. Liu (NRC, Canada)

* (now at UCLA, USA)

THz Applications – imaging, spectroscopy, sensing

- Remote Sensing of Earth's atmosphere, Astronomy
  - Terahertz range corresponds to rotational/vibrational energy levels in molecules, which tend to have a large radiative dipole moment (eg. OH (2.510 THz and 2.514 THz) and OH2 (2.503 THz) monitored by NASA EOS-Aura satellite to study ozone layer formation).
  - Study of early universe and galaxy formation – cool (30K) interstellar dust
- Security applications – weapon detection, package inspection, drug and explosive detection
- Terahertz imaging for medical applications – e.g. sub-dermal carcinoma detection based on differences in water content of tumor
- Chemical gas sensing, agent detection
- Biological sensing – stretching and twisting modes in DNA. These low-frequency modes are associated with specific species.
- End-point detection in dry-etching processes
- Plasma diagnostics in fusion experiments
- ...

THz spectroscopy for drug detection

(K. Kawase, RIKEN Japan, OPN, October 2004)

Three different drugs, MDMA (left), aspirin (center), and methamphetamine (right), have different images in T-rays.

Pictures taken with a THz OPO (1.3-2 THz) and mechanical scans (scan time ~10 minutes).

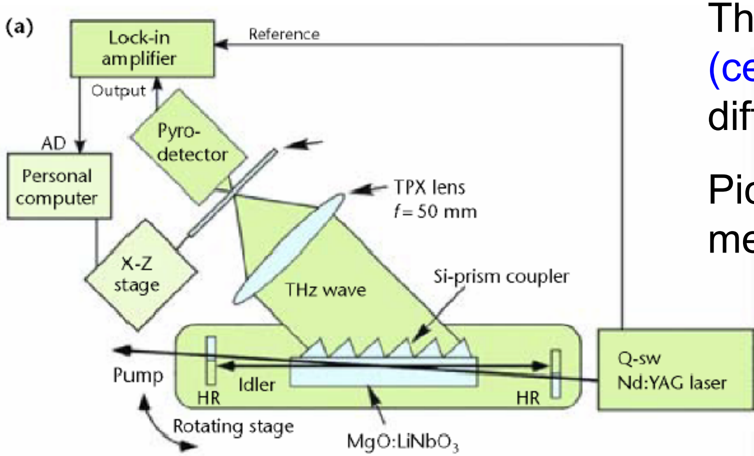

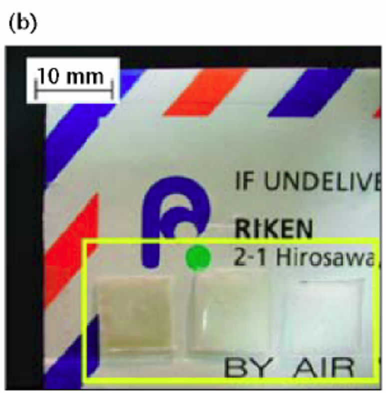

Figure 1. (a) Schematic of THz spectroscopic imaging system using THz wave parametric oscillator. (b) View of the samples. The small polyethylene bags contain (*left to right*): MDMA, aspirin and methamphetamine. The bags were placed inside the envelope and the area indicated by the yellow line was scanned.

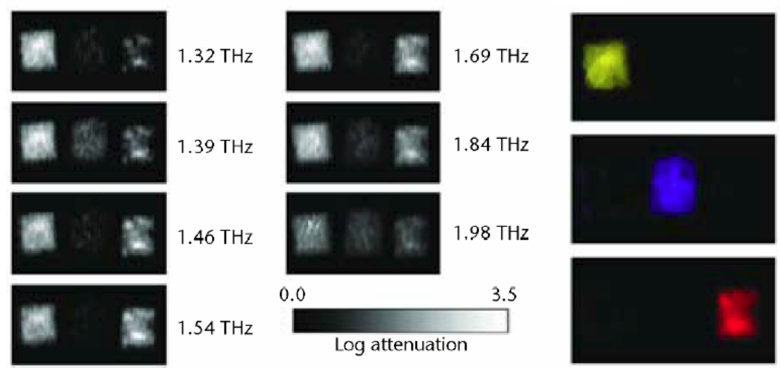

Figure 2. (a) Multispectral image of the target, recorded at seven frequencies between 1.32 and 1.98 THz. (b) Spatial patterns of MDMA (*yellow*), aspirin (*blue*) and methamphetamine (*red*) extracted from the multispectral image by use of fingerprint spectra.

Low frequency THz QCLs: Motivation

Very low atmospheric absorption near 1.5 THz

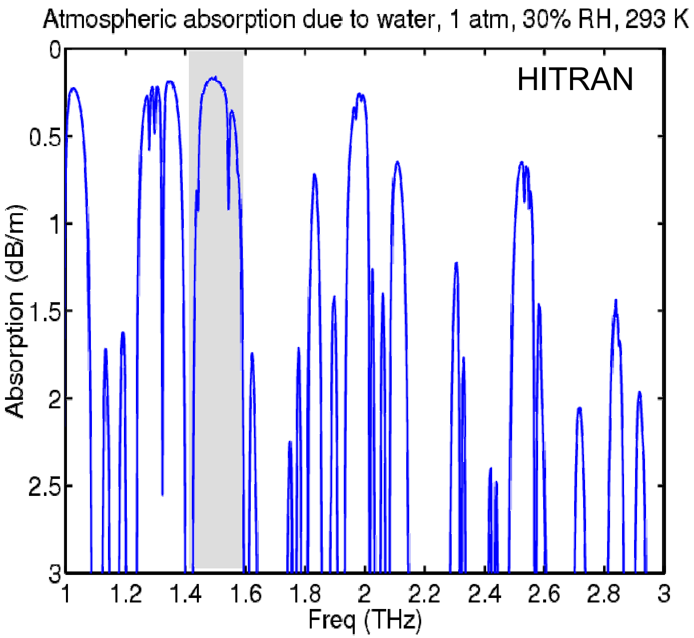

Image taken with a 1.56 THz transceiver system (FIR gas laser and Schottky diode mixer) in ~7 minutes at a standoff distance of 2 meters

Dickinson *et al.*, DSS 2006

THz (T-ray) imaging for medical applications

1st Medical Application: THz Imaging of Basal Cell Carcinoma in-vivo by TeraView

T-Ray Imaging is being applied for the first time to medical diagnostics

Below: In Vivo and Ex Vivo imaging of Basal Cell Carcinomas using the transportable TPI System developed by TeraView Ltd.

(slide courtesy Don Arnone, Teraview Ltd.)

In vivo TPI™ images of basal cell carcinoma recorded with TPI scan

BCC on upper forearm *TPI shows buried tissue*

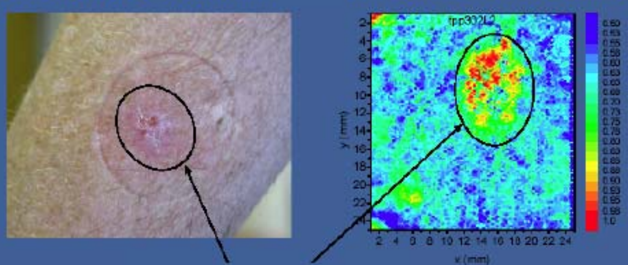

Tumor

Ex vivo TPI™ images of basal cell carcinoma recorded with TPI scan

Visible picture of patient forehead with suspect lesion

Uniform low absorption (green) by healthy tissue

TPI image

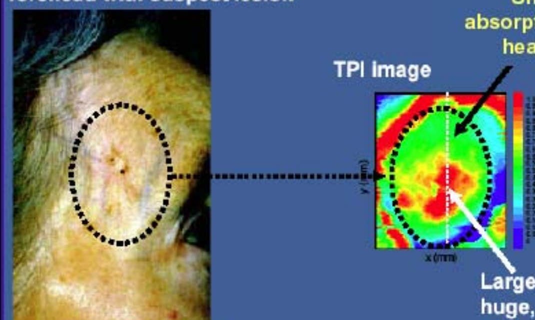

Where is the lesion?

Large 'hot spots' show huge, invisible tumour under surface of skin

TeraView
Realising potential

The terahertz gap

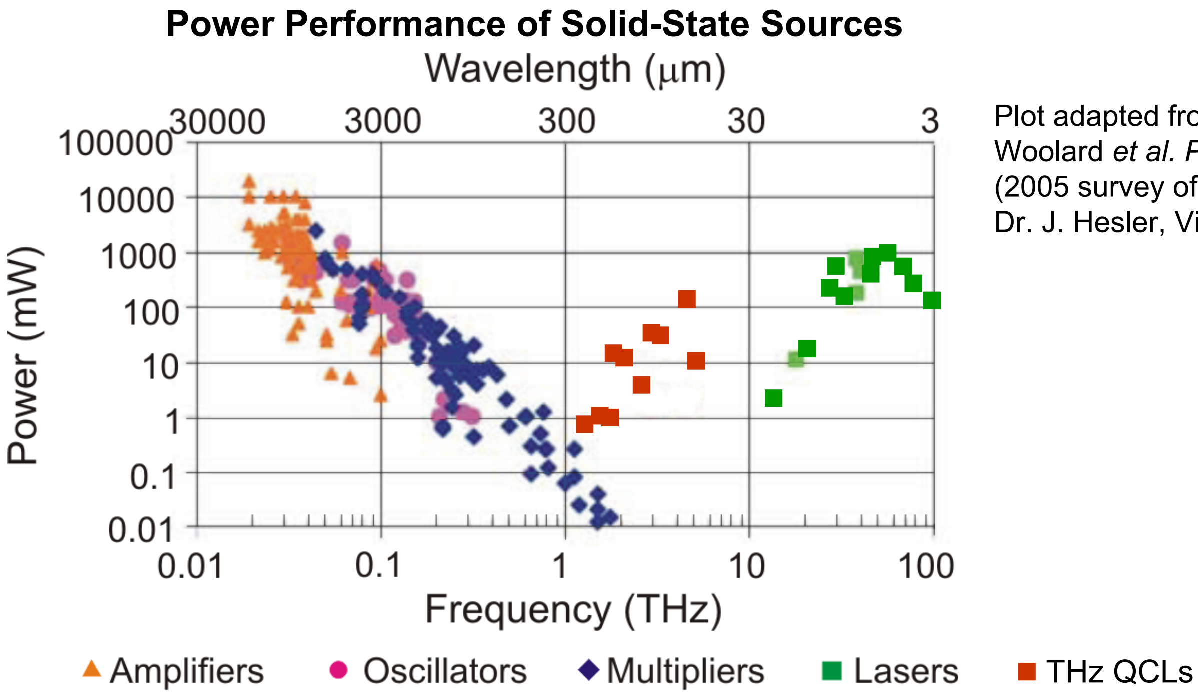

Plot adapted from:
Woolard *et al. Proc. IEEE* **93**:1722 (2005)
(2005 survey of THz sources,
Dr. J. Hesler, Virginia Diode Inc.)

THz Quantum Cascade Lasers:

- 1.2–5.0 THz
- CW Power ~ 1–140 mW (10 K)
- Peak operating temperature:
  169 K (pulsed), 117 K (cw)

Waveguides for THz QCLs

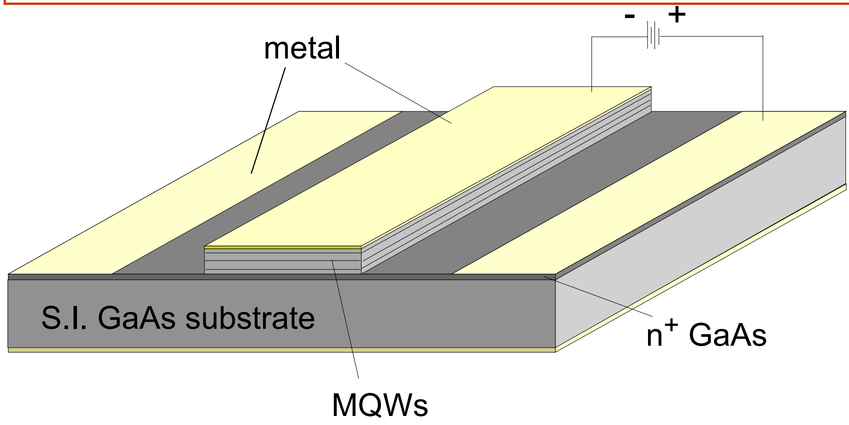

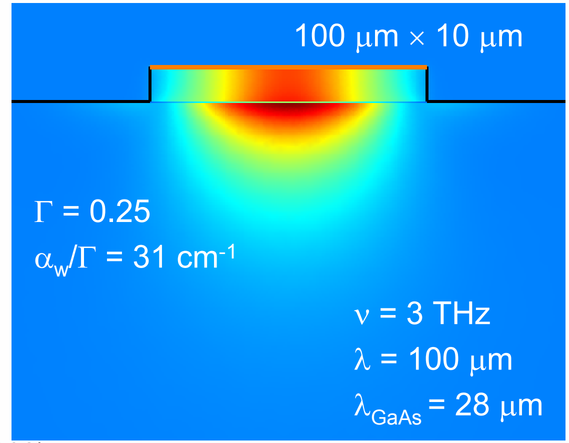

Semi-insulating surface-plasmon waveguide

R. Köhler *et al.*, Nature, **417**, 156 (2002)

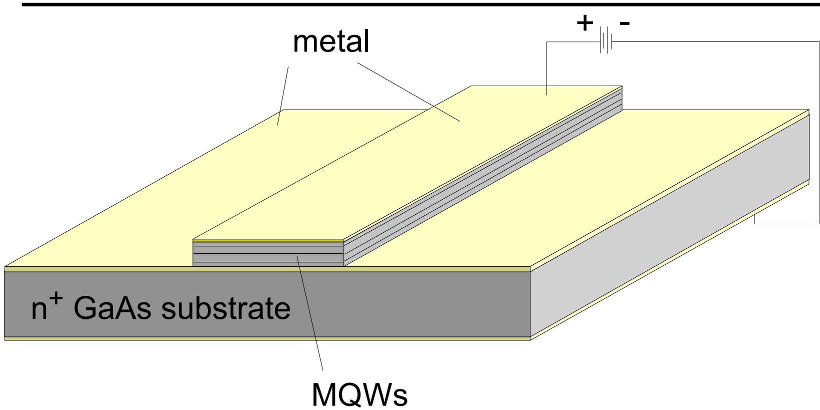

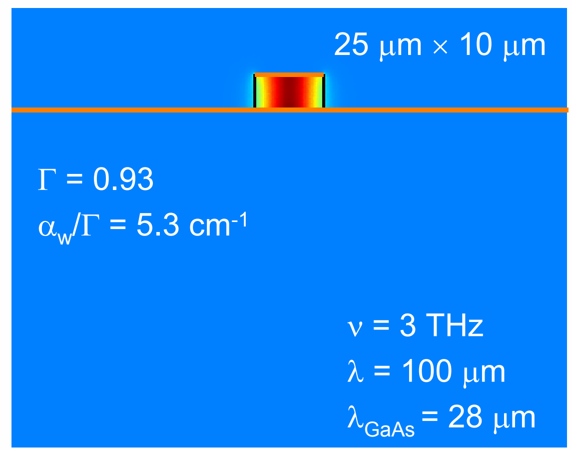

Metal-metal waveguide

B. S. Williams, S. Kumar, H. Callebaut, Q. Hu, and J. L. Reno, Appl. Phys. Lett., **83**, 2124 (2003)

THz QCL active region design

A simple 3-level THz QCL design

Operating (design) bias

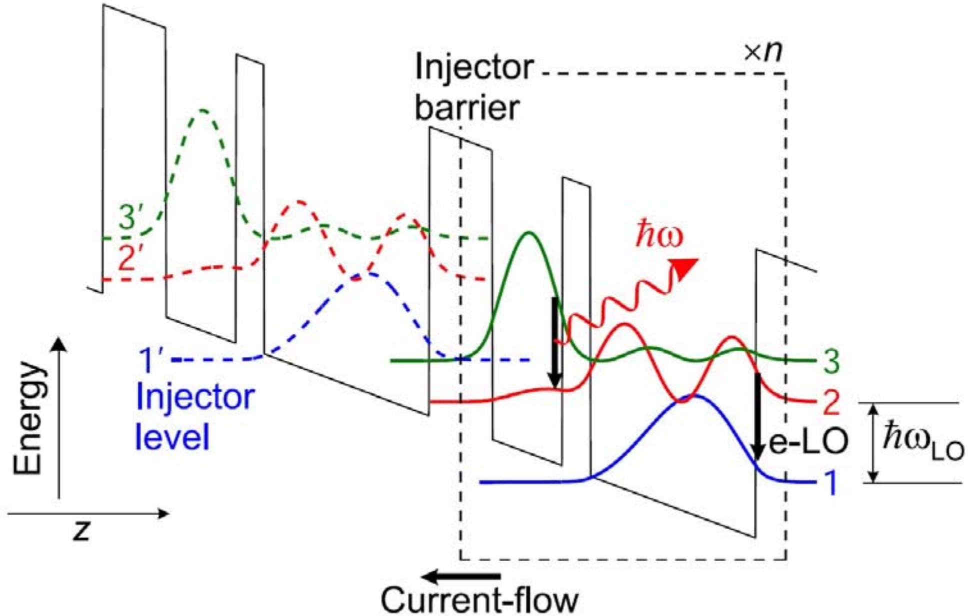

Peak Intersubband gain:

$$g_{\text{peak}} \propto \frac{f_{32}\Delta n}{\Delta \nu}$$

Population inversion:

$$\Delta n \propto \tau_3 \left(1 - \frac{\tau_2}{\tau_{32}}\right)$$

- f_{32} – oscillator strength ($\propto |z_{32}|^2$ (dipole-matrix element))
- Δn – population inversion ($= n_3 - n_2$)
- $\Delta \nu$ – linewidth of intersubband transition

Resonant-phonon depopulation scheme

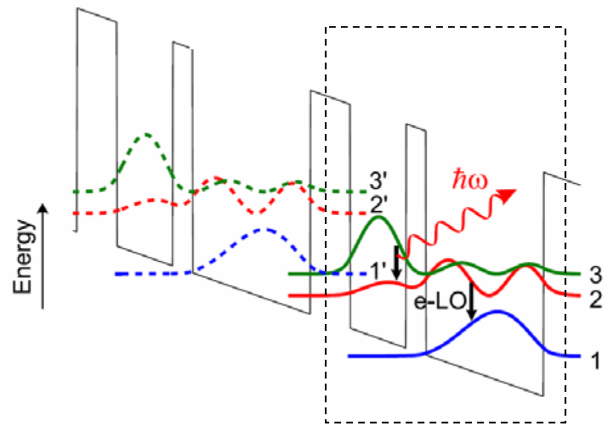

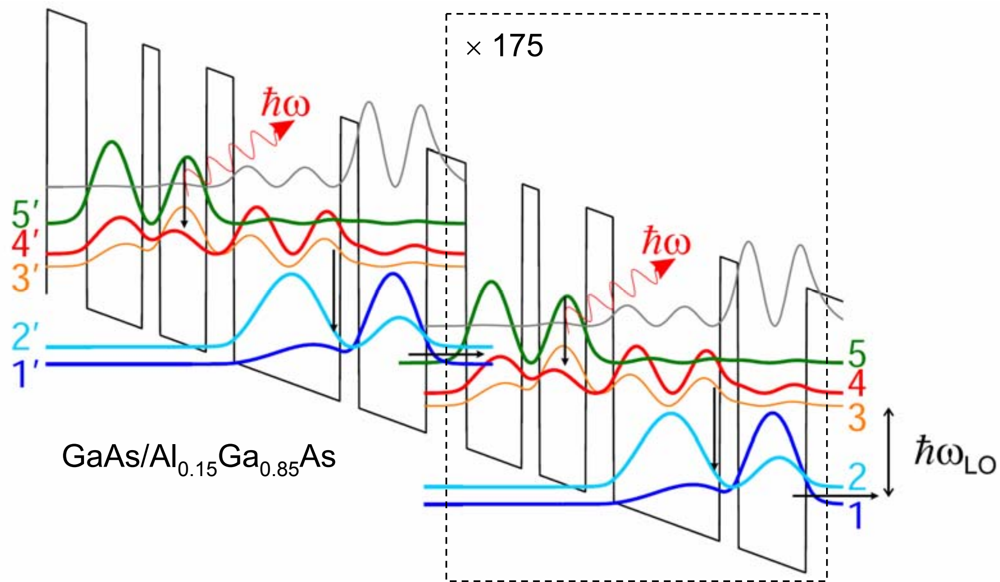

The simple 3-level *model* design → A radically improved 5-level design

- Radiative transition has to be kept very diagonal to maintain a long upper state lifetime, i.e. a small oscillator strength

- Radiative transition is vertical between levels 5 and 4, yielding a large oscillator strength of $f_{54} \approx 0.8 - 1.0$.
- At the designed bias, level 4 is at resonance with level 3, enabling a very fast ($\tau_4 \approx \tau_3 \sim 0.5$ ps) depopulation scattering, while keeping the upper level's lifetime relatively long ($\tau_{5\rightarrow 2,1} \approx 7$ ps).

B. S. Williams, H. Callebaut, S. Kumar, Q. Hu, and J. L. Reno, Appl. Phys. Lett., **82**, 1015 (2003)

Electrical transport behavior: the low-bias parasitic current channels

Design bias

2’ → 5, 1’→5

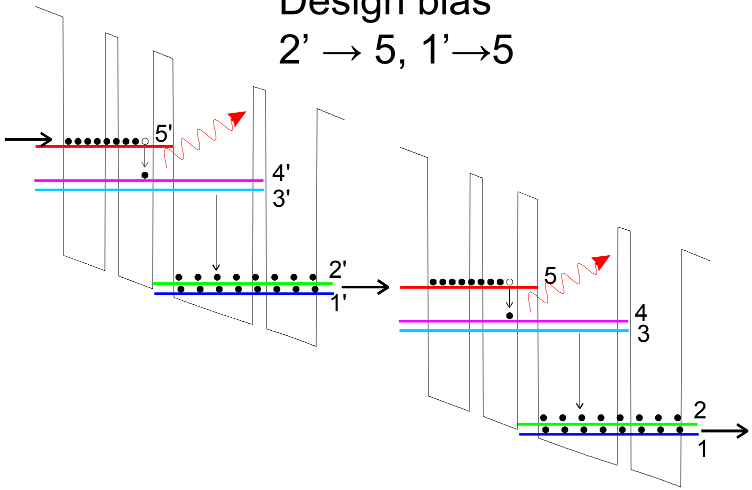

Parasitic bias

2’→3, 1’→3

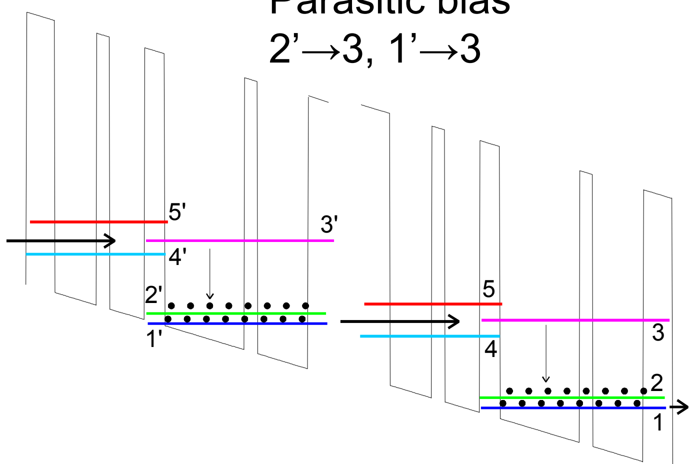

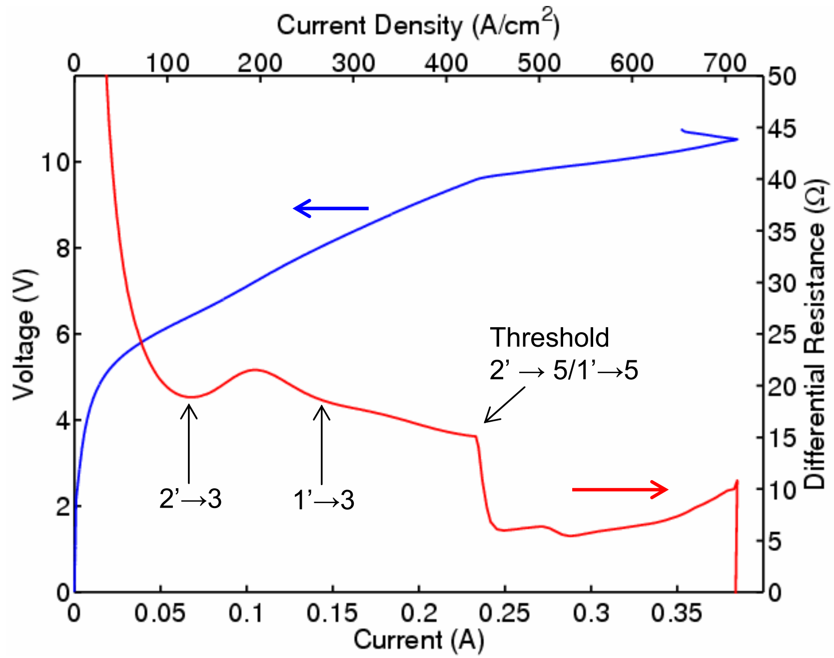

- Parasitic current channels artificially enhance $J_{threshold}$, however, reducing $J_{parasitic}$ tends to reduce J_{max}
- J_{max}- $J_{threshold}$ maximized by injector design

Experimental results for the 5-level design (with metal-metal waveguides)

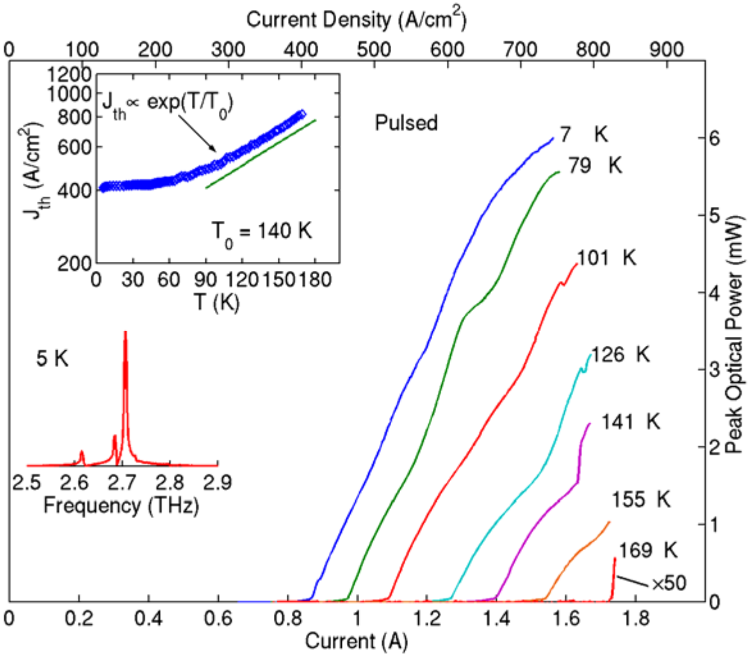

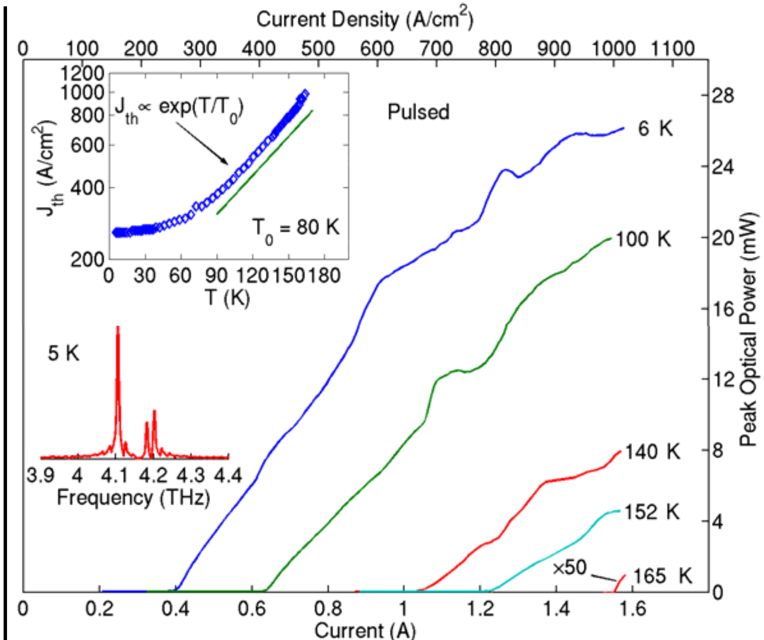

- ν=2.7 THz, T_{max} = 169 K (Pulsed)
- 100-μm wide, 2.10-mm long ridge, metal-metal waveguide
- Peak power = 6 mW (10 K)
- $k_B T_{max} \approx 1.2 \times \hbar\omega$, a value that is unprecedented for any solid-state photonic device

- ν=4.2 THz, T_{max} = 165 K (Pulsed)
- 80-μm wide, 1.94-mm long ridge, metal-metal waveguide
- Peak power = 26 mW (10 K)

Experimental results for the 5-level design (with metal-metal waveguides)

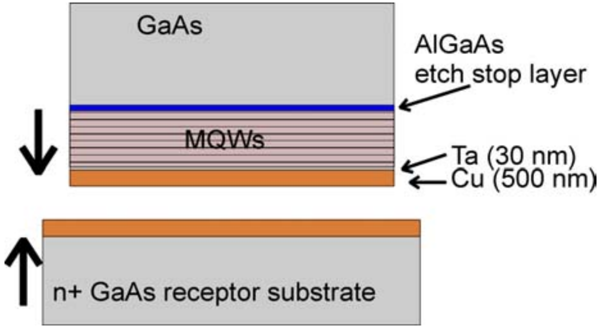

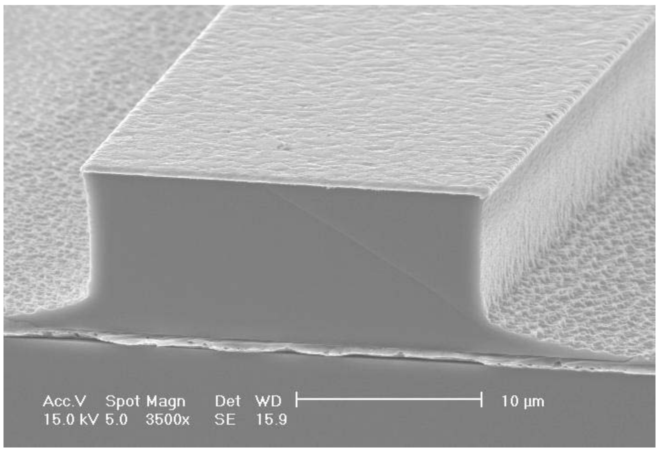

Cu-Cu thermocompression bonding: good thermal/electrical conductivity, improved bond quality

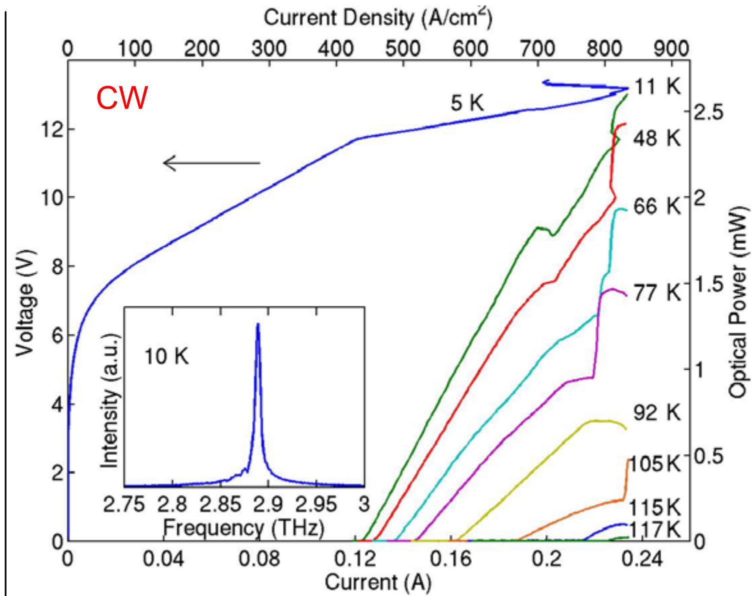

- T_{max} = 117 K (CW)
- 23-μm wide, 1.22-mm long ridge: width/λ ~ 0.22
- CW power dissipation ≈ 1-2 W (as compared to ≈ 20-50 W for our earliest lasers in SISP waveguides)
- Still >1 mW power at 78 K

B. S. Williams, S. Kumar, Q. Hu, and J. L. Reno, Optics Express, **13**, 3331 (2005)

A one-well injector design for lower frequencies

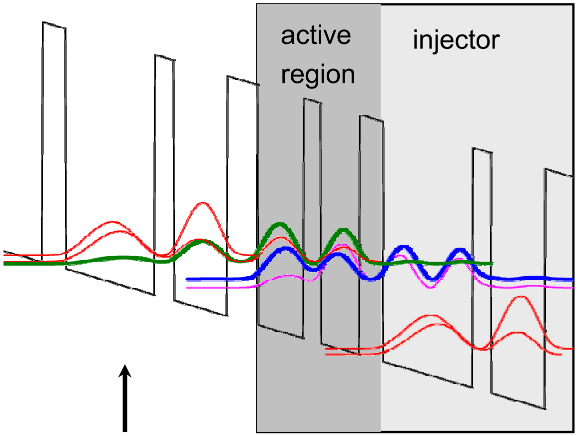

Original two-well injector design (5-levels/module)

One-well injector design (4-levels/module)

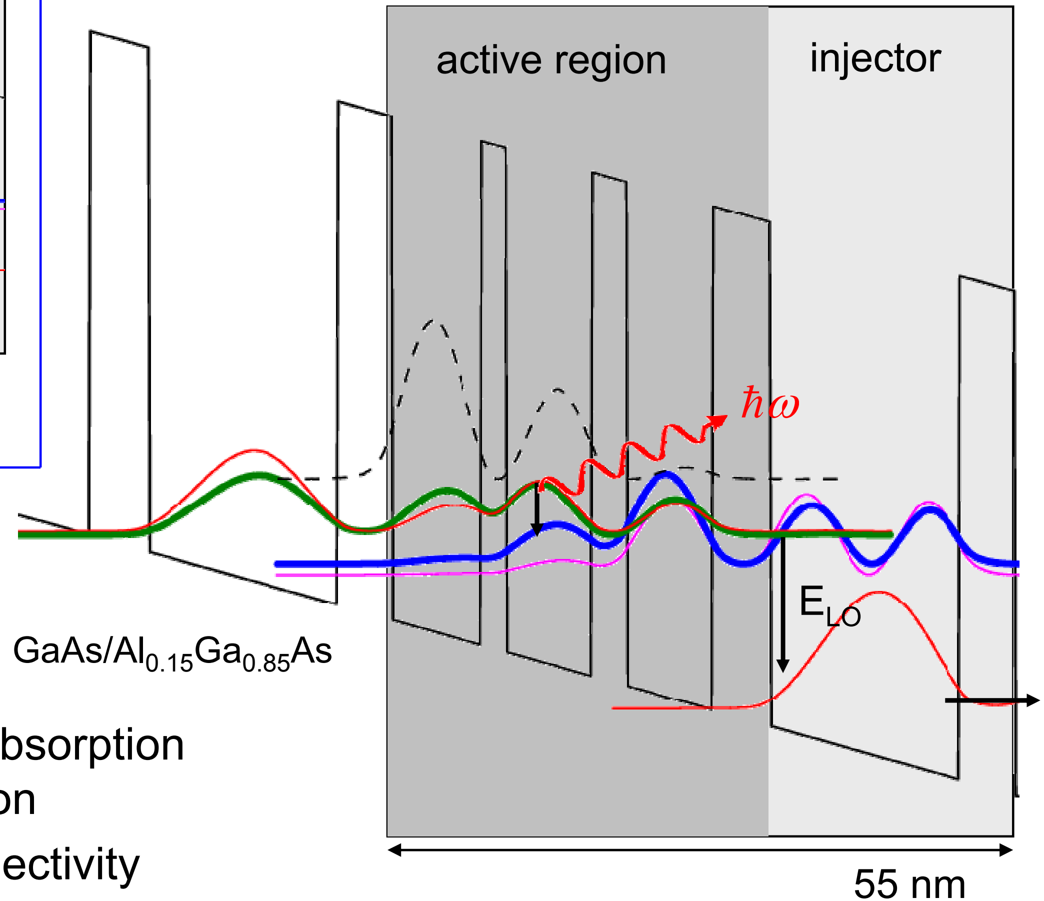

- Lower intersubband absorption loss in the active region
- Improved injection selectivity

S. Kumar, B. S. Williams, Q. Hu, and J. L. Reno, Appl. Phys. Lett., **88**, 121123 (2006)

1.9 THz QCL

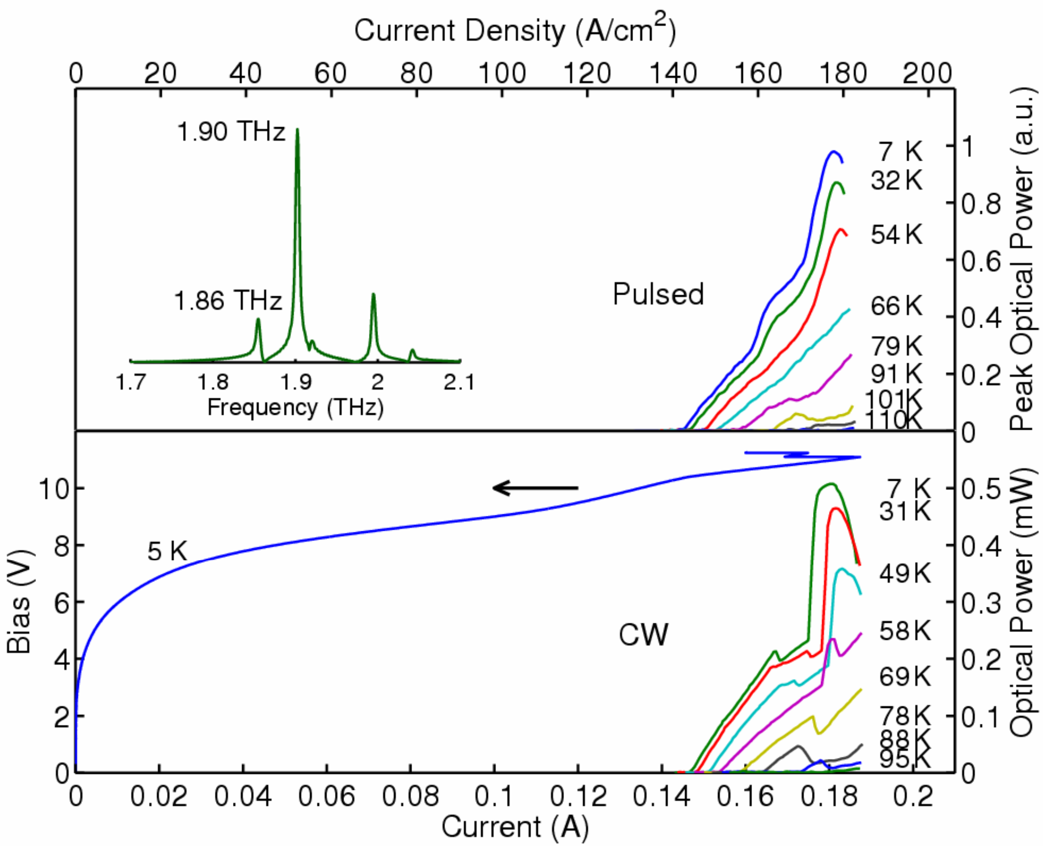

97-μm x 1.05-mm ridge, metal-metal waveguide

- J_{th} ~ 140 A/cm² at 5 K, the lowest of all published resonant-phonon THz QCLs
- $k_B T_{max} \approx 1.2 \times \hbar\omega$
- CW T_{max} = 95 K

S. Kumar, B. S. Williams, Q. Hu, and J. L. Reno, Appl. Phys. Lett., **88**, 121123 (2006)

Electrical transport behavior for the 1.9 THz QCL

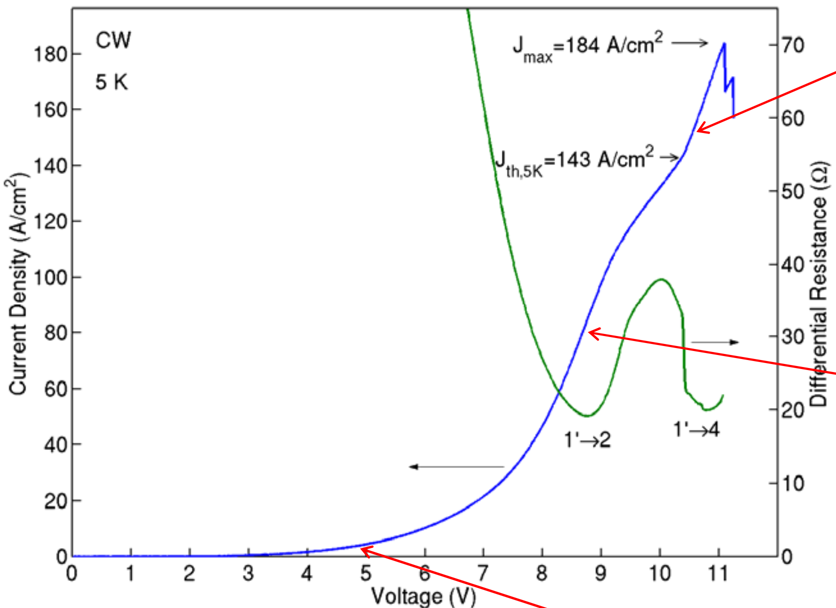

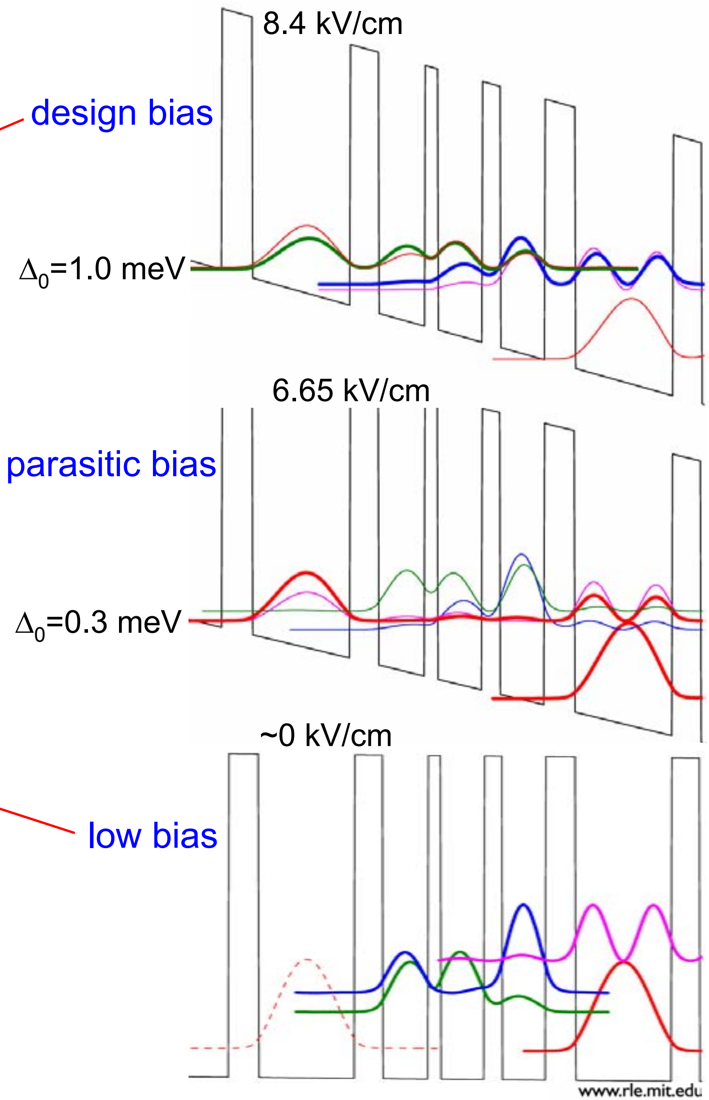

Measured I-V, $\frac{dV}{dI}$-V characteristics

1.6 THz QCL

Spectrum

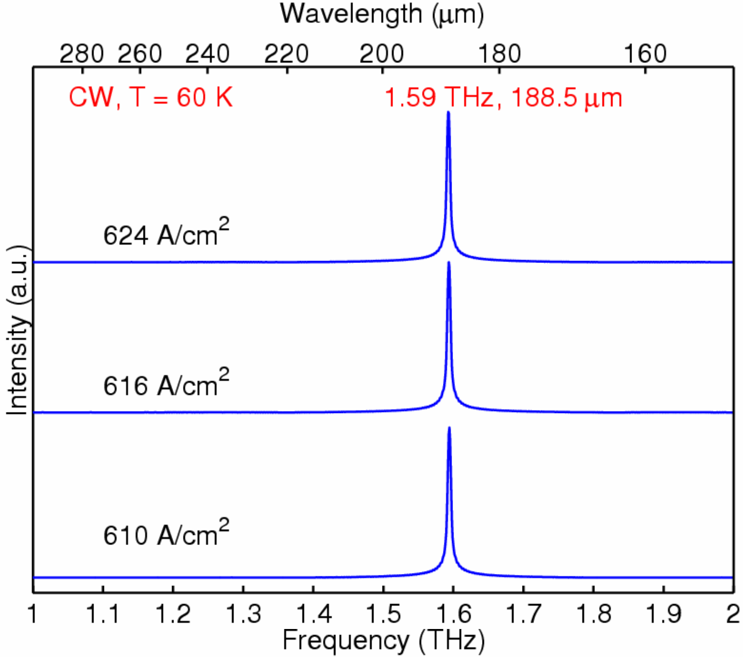

CW L-Is and I-V

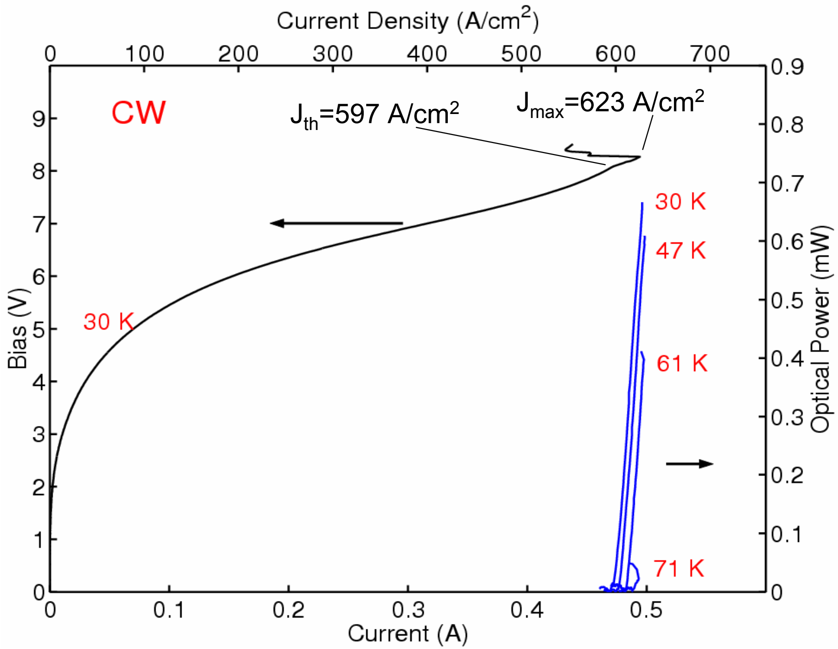

76-µm x 1.04-mm ridge, metal-metal waveguide

- CW T_{max} = 71 K

1.4 THz QCL (a modified one-well injector design)

Spectrum

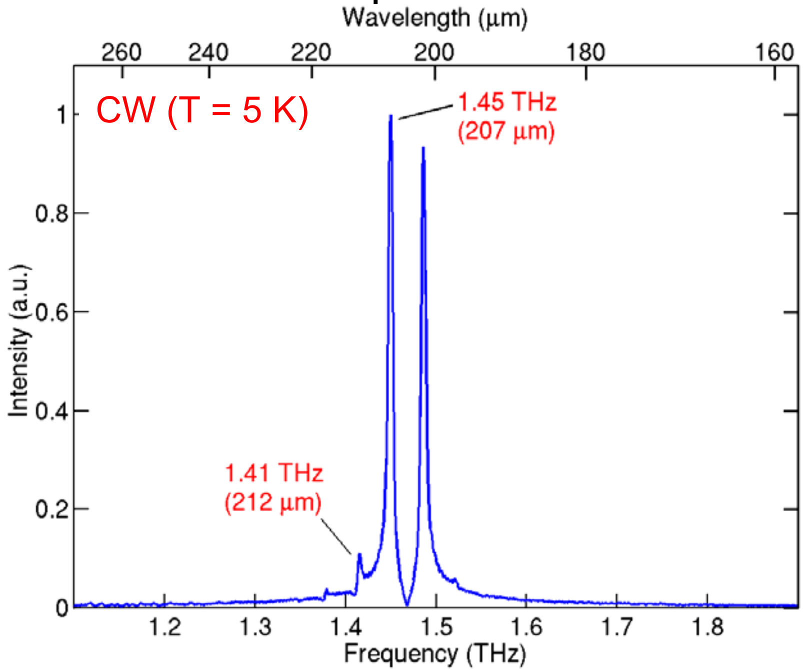

CW L-Is and I-V

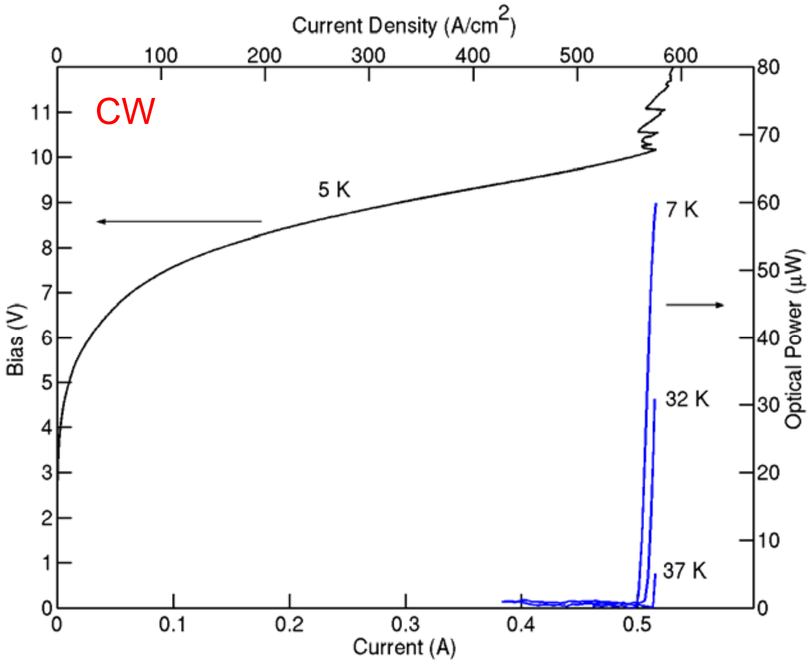

80-μm x 1.12-mm ridge, metal-metal waveguide

- CW T_{max} = 37 K

- For one-well injector QCLs the low-bias parasitic current channel, and not free-carrier losses, is expected to challenge operation at even lower frequencies

Sub-THz lasing in the 5-level design with magnetic field

A. Wade, D. Smirnov *et. al.* (2007) – see the talk at 10:20AM, Wednesday

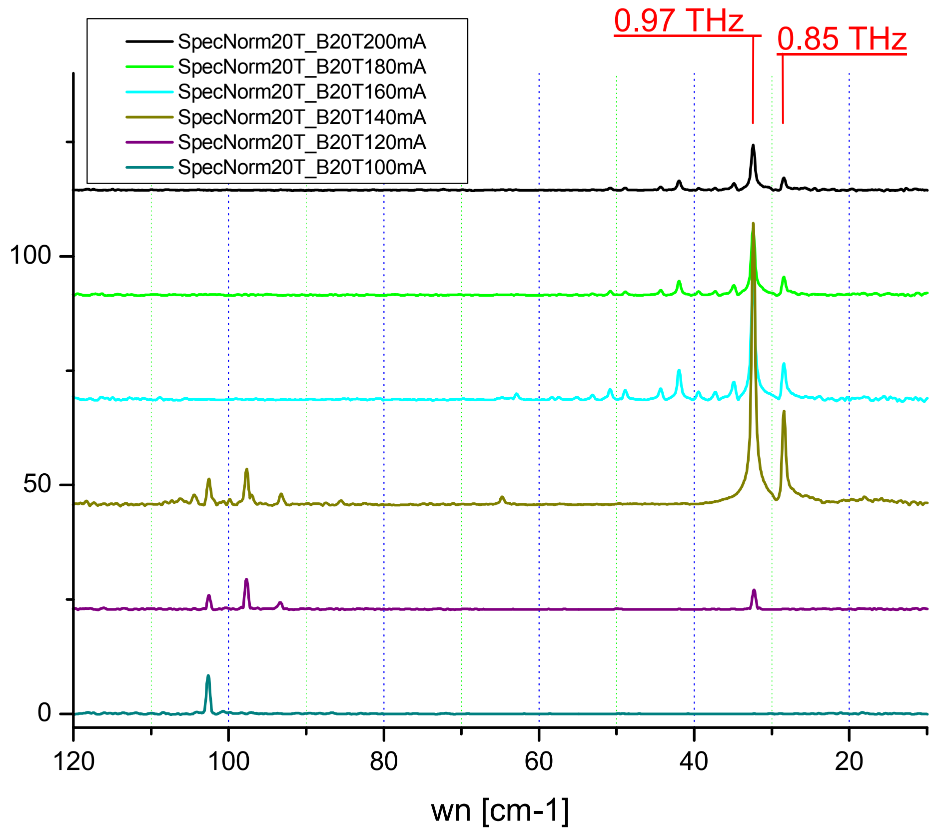

- Lasing at ν ~ 0.85 THz, corresponding to λ ~ 353 μm.

Summary

- Resonant-phonon depopulation + metal-metal waveguides has provided a robust platform for high-temperature as well as low-frequency operation
- Record high operating temperatures of 117 K (cw) and 169 K (pulsed)
- Operating frequencies from 1.4 – 5.0 THz (down to 0.85 THz with magnetic field)
- Higher temperature operation is currently limited by dynamic range between parasitic channel and peak current density.
- Low frequency operation is also limited by the low-bias parasitic current channels rather than optical losses in the active region

- Future
  - Higher temperature operation – TE cooled? Room temp?
  - Lower frequency operation – below 1 THz without magnetic field?